Low-Temperature Rheological Behavior and Wax Deposition Control in High-Paraffin Blended Crude Oils Using Chemical Additives

A. V. Gasimzade[a,*] and V. Kh. Nurullayev[b]
[a]Azerbaijan State Oil and Industry University (ASOIU)
[b]SOCAR Pipeline Department

doi: https://doi.org/10.15255/CABEQ.2026.2479

Original scientific paper
Received: January 20, 2026
Accepted: April 21, 2026

This study investigates the low-temperature rheological behavior and wax deposition tendency of high-paraffin blended crude oil in order to improve flow stability during pipeline transportation. The results show that decreasing temperature leads to a significant increase in yield stress and effective viscosity, indicating the formation of a structured paraffin network responsible for reduced flowability. Comparative analysis demonstrated that the Herschel–Bulkley model most accurately describes the non-Newtonian behavior of the system ($R^2 = 0.995$). Strong correlations between pour point, yield stress, and consistency index confirm the structural origin of flow resistance and highlight the role of crystallization processes in determining rheological properties.

Chemical treatment significantly weakened intermolecular interactions within the paraffin–resin–asphaltene system, reduced wax deposition tendency, and improved flow characteristics. Among the investigated formulations, the composite additive (DHC) exhibited the highest efficiency, promoting partial transition toward near-Newtonian behavior and enhanced low-temperature mobility. The results demonstrate that composite chemical additives provide an effective approach for controlling structure formation and improving transportation properties of high-paraffin crude oils.

Keywords
rheology, yield stress, wax deposition, flow behavior index, chemical additives

Introduction

The structural behavior of high-paraffin blended crude oils is governed by the combined effects of paraffin, asphaltene, and resin components, which together form a complex and continuously evolving system. As temperature decreases or shear rate is reduced, paraffin crystals begin to precipitate and gradually interconnect, leading to the formation of spatial network structures within the oil. As a result, the rheological behavior deviates from Newtonian flow: the linear relationship between shear stress and shear rate is lost, a yield stress (τ_0) emerges, and the effective viscosity increases sharply[1,2].

High concentrations of asphaltenes and resins further intensify this behavior by forming stable adsorption layers around paraffin crystals, thereby reinforcing the internal structural network. Strong intermolecular interactions between the dispersed phase and the surrounding medium accelerate the transition of the system toward a gel-like state. Under flow conditions, this structural arrangement results in pronounced resistance to deformation, while upon cessation of shear, the structure may partially or fully recover, reflecting the time-dependent nature of the system. In current production and transportation practices, the significance of these phenomena has increased due to the declining availability of light crude oils and the growing production of heavy and high-paraffin crudes[3]. During pipeline transportation, disturbances in thermal and hydrodynamic conditions frequently promote paraffin deposition, increase hydraulic resistance, and reduce flow stability. These effects ultimately lead to decreased transportation efficiency, higher energy demand, reduced pipeline throughput, and diminished operational reliability[4–7]. The complexity is further amplified when multiple crude oils are blended. Studies indicate that the composition of crude oil produced from one well differs from that of another well within the same reservoir, and even successive productions from the same well are not compositionally identical. Consequently, the blending of high-paraffin crudes with differing compositions more strongly manifests in variations in rheological behavior, flow rates, and the tendency toward structure formation. Considering that crudes of different compositions are typically collected in

*Corresponding author:
qasimzade92@inbox.ru, aysel.qasimzade@asoiu.edu.az

storage tanks after treatment prior to transportation, the occurrence of such mixing-induced complexities becomes nearly unavoidable[8–12]. For these reasons, a detailed investigation of the rheological properties of high-paraffin crude oils, improved understanding of structure formation mechanisms, and the development of effective physicochemical flow control strategies are essential to ensure the safe and efficient operation of pipeline transportation systems[13–16].

Rheological models

High-paraffin oils can be regarded as structurally sensitive dispersed systems whose flow behavior is strongly influenced by temperature and shear conditions. Under such circumstances, the formation of paraffin-based structural network frameworks leads to non-Newtonian flow behavior and a significant increase in viscosity[17–19].

The aggregation of paraffin crystals, together with their interactions with resin–asphaltene components, enhances the mechanical strength of the internal structure and gives rise to yield stress. As a result, flow does not occur until a critical stress threshold is exceeded. This type of behavior is well described by the Bingham plastic model, which assumes a finite yield stress followed by an approximately linear flow response once the structure is disrupted[20–24].

At higher shear rates, the internal network progressively breaks down, leading to a reduction in flow resistance. In this regime, the flow behavior can be represented using the Power-law (Ostwald–de Waele) model, which captures the shear-dependent viscosity characteristic of pseudoplastic fluids but does not explicitly account for yield stress effects[25–27].

For a more realistic description of high-paraffin blended oils, the Herschel–Bulkley model provides a more flexible and physically meaningful framework. By incorporating both yield stress and nonlinear shear dependence, this model reflects the presence of paraffin-induced structural networks and their progressive destruction under shear, enabling a more accurate representation of the actual flow behavior of these systems[28–31].

Research method

Research objects

For the experimental investigation, a high-paraffin blended crude oil sample was prepared under laboratory conditions by blending crude oil samples collected from several wells of the Palchig–Pilpilasi oil field. The use of a blended crude oil allowed the reproducible evaluation of rheological and deposition behavior under controlled conditions. The physicochemical properties of the prepared oil sample are summarized in Table 1.

As observed from the table, the crude oil sample exhibits a high paraffin content. This characteristic is a major factor contributing to the operational challenges encountered during its transportation.

For the purpose of the present study, two types of depressor additives were employed — Difron-3971 and HY-154 reagents. The physicochemical characteristics of both reagents are presented in Tables 2 and 3.

A composite formulation, conditionally designated as DHC, was prepared under laboratory conditions for use in the experimental program. The composition of the formulation was as follows: Difron-3971 (25 wt%), HY-154 (6 wt%), kerosene (55 wt%), and xylene (14 wt%).

The components were mixed at ambient temperature (20–22 °C) using mechanical stirring at 2000 rpm for 10 min until a homogeneous solution was obtained. No additional surfactants or stabilizing agents were used. The prepared DHC composite was applied in rheological and wax-deposition experiments at specified dosages. Prior to each experiment, the formulation was gently homogenized to ensure uniform distribution of active components.

Experimental methods

Separation of paraffins, asphaltenes, and resins

The separation of paraffins, asphaltenes, and resins (SARA fractions) from crude oil was carried out according to standardized procedures based on GOST 11858 and GOST 11851, with methodological approaches comparable to ASTM D2007 and IP 143 fractionation methods.

Initially, 3–5 g of crude oil sample was mixed with n-heptane at a ratio of 1:40 (v/v) and kept for 16 h to ensure complete precipitation of asphaltenes. The precipitated asphaltenes were separated by filtration.

The remaining maltene fraction was subjected to adsorption chromatography for separation of resins and paraffins. Desorption of resins was performed using an alcohol-toluene mixture. The obtained paraffin-containing solution was distilled to remove solvents and subsequently mixed with an acetone-toluene solution (35:65). The mixture was kept at –20 °C to induce paraffin crystallization. The precipitated paraffins were separated by vacuum filtration using a temperature-controlled cooling bath.

Table 1 – *Physicochemical properties of the high-paraffin blended crude oil sample*

№	Indicator	Value	Test method
1	Density at 20 °C, kg m^{-3}	901.0	ASTM D1298 / GOST 3900-85
2	Resin content, wt.%	4.3	GOST 11858-66
3	Asphaltene content, wt.%	0.18	ASTM D6560 / GOST 11858-66
4	Paraffin content, wt.%	15.2	GOST 11851-85

Table 2 – *Physicochemical characteristics of the depressor additive Difron-3971*

Indicator	Value
Appearance, color	Viscous yellow liquid, aromatic odor
Density (at 15 °C)	0.850 – 0.930 g cm^{-3}
Pour point	< 10 °C
Melting point	38 – 40 °C
Flash point (closed cup)	> 60 °C
Solubility	Soluble in hydrocarbon solvents, insoluble in water

Table 3 – *Physicochemical characteristics of the depressor additive HY-154*

Indicator	Value
Appearance	Brown viscous liquid
Kinematic viscosity (at 100 °C)	150–250 mm^2 s^{-1}
Total base number (TBN)	15–30 mg KOH g^{-1}
Flash point (COC)	≥ 170 °C
Nitrogen content	1.1–1.3 wt.%
Density (at 20 °C)	0.89–0.94 g cm^{-3}
Color (chromaticity, diluted)	≤ 7.0
Water content	≤ 0.10 wt.%

The applied procedure ensures reproducible fractionation of structural components responsible for rheological behavior and wax deposition tendency of paraffin-containing crude oils[32–35].

Determination of kinematic viscosity

Kinematic viscosity was measured using an Unbeholden-type capillary viscometer in accordance with GOST 33-2016. Temperature control was provided by a Labo Visco TV-2000 thermostatic bath (Arnhem, Netherlands) with an accuracy of ±0.1 °C.

Prior to measurements, the viscometers were thoroughly cleaned, dried, and filled with the test sample. The filled viscometer was placed in the thermostatic bath and equilibrated for 15 min to ensure thermal stability. The flow time of the liquid between two calibrated marks was then recorded. Each measurement was repeated 3–4 times, and the relative deviation between parallel measurements did not exceed 0.6 % [34–37].

Determination of effective viscosity and shear stress

Effective viscosity and shear stress were measured using a Brookfield rotational rheometer in accordance with GOST 1929-87. The measurements were conducted with a cylindrical MK-CC45 system over a shear rate range of 5–120 s^{-1}, at temperatures of 0, 5, 10, 15, and 20 °C. Temperature and shear rate were controlled by a dedicated program (RHEO 2000, version 2.6). Each measurement was repeated three times, and the relative deviation between parallel measurements did not exceed 1.5 % [34–39].

Inhibition of asphaltene–resin–paraffin deposits (cold finger method)

The inhibition of asphaltene–resin–paraffin deposits (ARPD) was investigated using the "cold finger" method in a specially designed apparatus. The experiment was performed in a 500 mL thermostatic cylindrical vessel made of stainless steel. A 300 mL oil sample was stirred magnetically and maintained at a given temperature. A cooled steel rod (3 °C) was immersed into the oil while the bulk oil temperature was reduced from 60 °C to 20 °C at a controlled cooling rate of 0.5 °C min^{-1}. Deposit formation was allowed to proceed for 4 hours. Afterwards, the rod was removed, washed with 50 mL of acetone, and the deposits were mechanically cleaned off. Each experiment was performed in triplicate, and mean values were reported. The relative standard deviation between parallel measurements did not exceed 2.5 %. The mass of the deposits was measured, and the inhibition efficiency was calculated according to the following formula (GOST, 1966; GOST, 1985)[32,33]:

$$W(\%) = \frac{m_0 - m}{m_0} \cdot 100 \quad (1)$$

where, m_0 is the mass of ARPD formed in the untreated oil (g), and m is the mass of ARPD formed in the oil treated with reagent.

Determination of pour point

The pour point was determined in accordance with GOST 20287-2023 and the corresponding regulatory documentation (RD-1982). Each measurement was repeated three times, and the mean value was reported. The deviation between parallel measurements did not exceed 1 °C [39].

Rheological modeling

The rheological behavior of the crude oil samples was analyzed using three widely accepted rheological models: the Bingham, Herschel–Bulkley, and Power-law models. These models were selected to compare linear, yield-stress-dependent, and nonlinear flow behaviors over the investigated shear-rate range.

Bingham model

The Bingham model assumes the presence of a yield stress, below which no flow occurs, followed by linear viscous behavior. It is expressed as:

$$\tau = \tau_0 + K_p \dot{\gamma} \tag{2}$$

where τ is the shear stress (Pa), τ_0 is the yield stress (Pa), K_p is the plastic viscosity (Pa s^n), and $\dot{\gamma}$ is the shear rate (s^{-1}).

Herschel–Bulkley model

The Herschel–Bulkley model extends the Bingham approach by accounting for nonlinear flow behavior after yielding and is given by:

$$\tau = \tau_0 + K \dot{\gamma}^n \tag{3}$$

where K is the consistency index (Pa s^n) and n is the flow behavior index. Values of $n < 1$ indicate shear-thinning behavior, while $n > 1$ corresponds to shear-thickening flow.

Power-law model

The Power-law model describes non-Newtonian flow without considering yield stress and is expressed as:

$$\tau = K \dot{\gamma}^n \tag{4}$$

This model was applied to evaluate the extent of shear-dependent viscosity and to compare its predictive capability with yield-stress-based models.

Parameter estimation

Model parameters (τ_0, μ_p, K, and n) were determined by nonlinear regression of the experimental shear stress–shear rate data obtained from rotational rheometry. The quality of the model fit was assessed by comparing correlation coefficients and the consistency of predicted trends across the investigated temperature range.

Results and discussion

The formation and accumulation of solid deposits represent one of the most evident indicators of structural development in high-paraffin oil systems. Monitoring the mass of deposits over time makes it possible to assess the intensity of paraffin crystallization, crystal aggregation, and adhesion to solid surfaces, as well as to evaluate the effectiveness of chemical reagents in inhibiting these processes. For this purpose, a comparative analysis of deposit growth behavior was carried out at a temperature of 30 °C for a reagent-free oil sample and for oil samples treated with different additives at various dosages. The results are presented in Fig. 1.

As observed in Fig. 1, the mass of solid deposits increased steadily with exposure time for all investigated systems, reflecting continuous paraffin crystallization and accumulation on the solid surface. The reagent-free oil sample consistently exhibited the highest deposit mass throughout the experiment, confirming its strong tendency toward structural buildup and surface adhesion. This behavior is associated with unrestricted growth and aggregation of paraffin crystals, resulting in the formation of a dense and structurally stable deposit layer.

The application of chemical reagents significantly reduced deposit formation over the entire time range. Among the tested systems, the DHC composite at a dosage of 600 g t^{-1} demonstrated the strongest inhibitory effect compared to the individual depressor additives, leading to the lowest deposit masses at all time intervals. This indicates that the DHC formulation effectively disrupted paraffin crystallization and interactions between paraffin crystals, thereby suppressing both nucleation and subsequent deposit growth.

Difron-3971 and HY-154 also markedly reduced deposit formation relative to the reagent-free oil sample, with higher dosages exhibiting improved performance. The observed dose dependence suggests that increasing reagent concentration enhances surface activity and strengthens the ability of additive molecules to interfere with paraffin crystal growth and aggregation. At the same time, the differences observed between Difron-3971 and HY-154 point to distinct interaction mechanisms with paraffin components, which may influence both deposit morphology and adhesion strength.

Despite the pronounced reduction in deposit mass, a gradual increase over time was still ob-

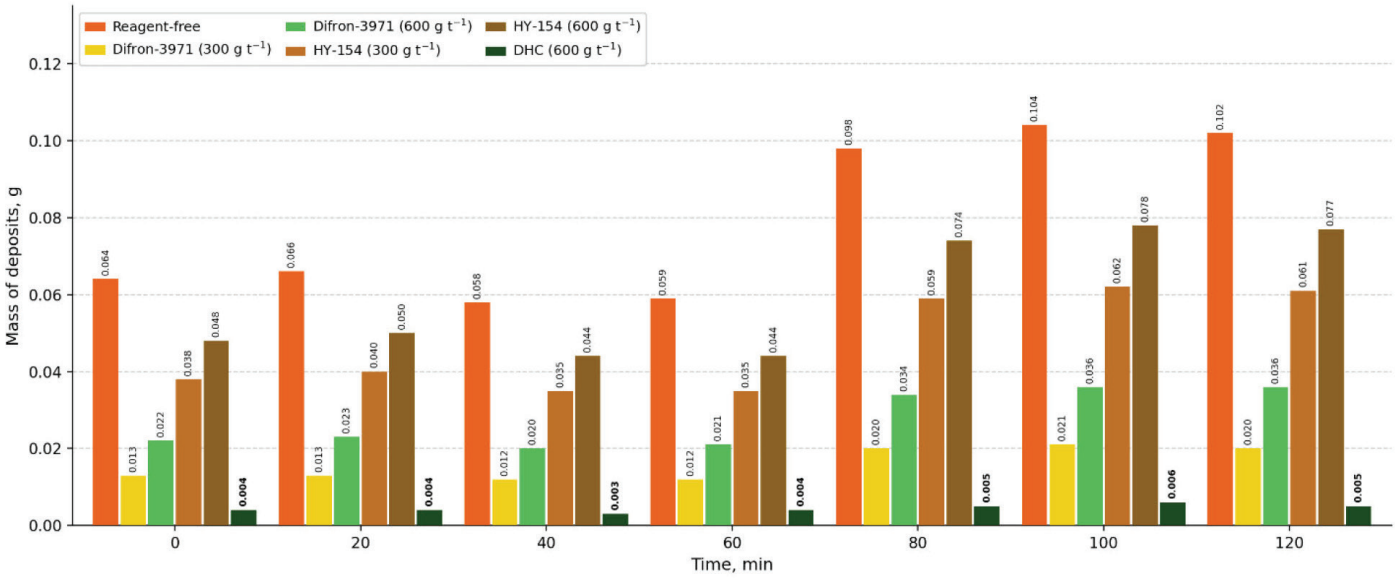

Fig. 1 – *Effect of different reagents and dosages on the mass of deposits as a function of time (T=30 °C)*

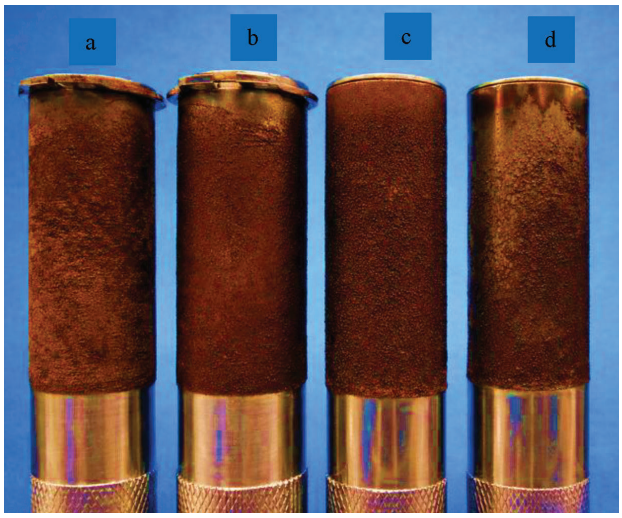

Fig. 2 – *Visual appearance of deposits formed on the surface of metal probes during the experiment; (a) reagent-free system; (b) Difron-3971 at 600 g t^{-1}; (c) HY-154 at 600 g t^{-1}; (d) DHC composite at 600 g t^{-1}*

served for samples with reduced deposition tendency, indicating that chemical additives slowed down—rather than completely prevented—structure formation. This observation is consistent with the previously discussed rheological results, where reduced yield stress and viscosity values reflected weakened but not fully eliminated structural networks. In this sense, the deposit mass can be regarded as a macroscopic manifestation of the same structural processes responsible for the non-Newtonian flow behavior of high-paraffin oil systems.

Experimental evidence confirms that chemical treatment provided an effective means of reducing deposit formation by modifying paraffin crystallization dynamics, with the DHC composite exhibiting the highest efficiency under the investigated conditions. Fig. 2 further supports these findings by providing a visual comparison of deposits formed on cold finger surfaces, clearly illustrating differences in the extent and morphology of solid-phase accumulation associated with structure formation in the high-paraffin blended crude oil.

As seen in Fig. 2, the lowest wax deposition was observed after the application of the DHC composite, confirming its superior efficiency in suppressing structure formation in the high-paraffin system.

Since the primary challenge during the transportation of high-paraffin oils is associated with flow behavior, further investigations were focused on the key rheological parameters governing flow[41]. Accordingly, the flow characteristics of the blended crude oil were examined in detail. The temperature dependence of the yield stress (τ_0) is presented in Fig. 3, highlighting the decisive role of thermal conditions and chemical treatment in controlling flow initiation in high-paraffin oil systems.

The results presented in Fig. 3 indicate that, for all investigated systems, the yield stress (τ_0) increased markedly as temperature decreased, reflecting the progressive development of a mechanically stable internal structure in high-paraffin oils. At higher temperatures, τ_0 values remained low or approached zero, indicating weak development or partial disruption of the paraffin crystal network, which allowed the oil to flow with relatively low resistance.

With decreasing temperature—particularly below a certain critical temperature range—a sharp increase in yield stress was observed. This behavior can be attributed to intensive paraffin crystallization and the formation of an interconnected three-di-

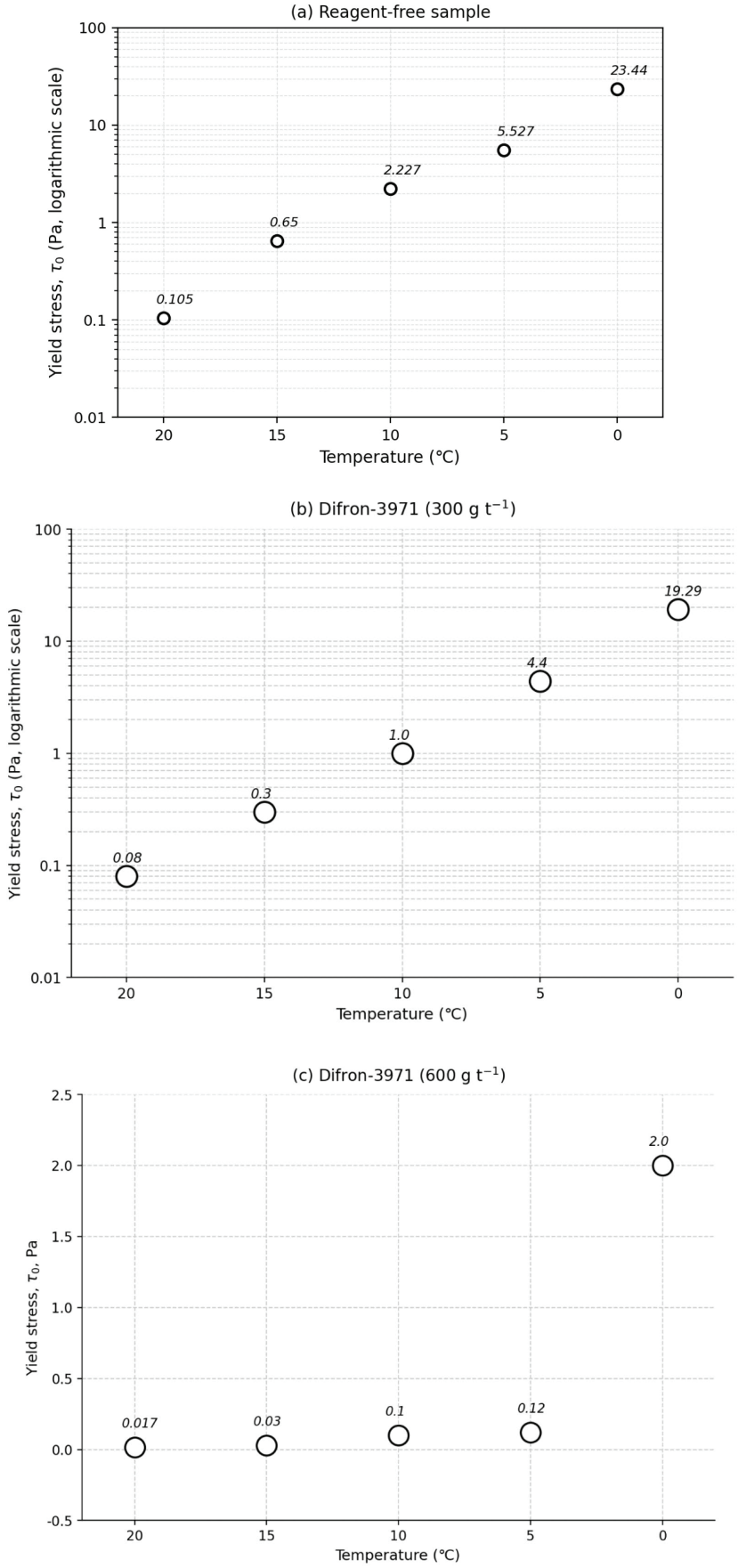

F i g . 3 – *Temperature dependence of yield stress (τ_0) for high-paraffin crude oil under different reagent conditions: (a) reagent-free sample; (b) Difron-3971 (300 g t^{-1}); (c) Difron-3971 (600 g t^{-1}); (d) HY-154 (300 g t^{-1}); (e) HY-154 (600 g t^{-1}); (f) DHC (600 g t^{-1})*

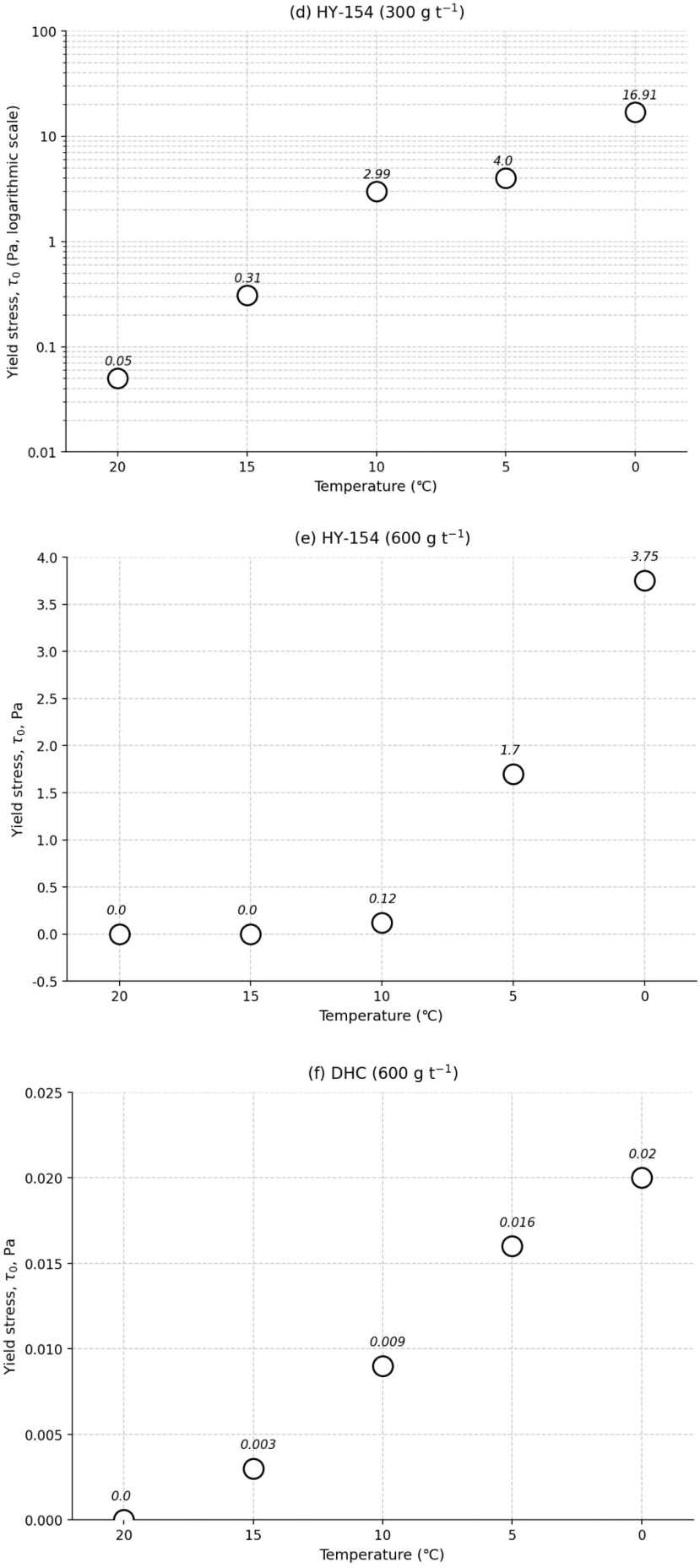

Fig. 3 – *continued*

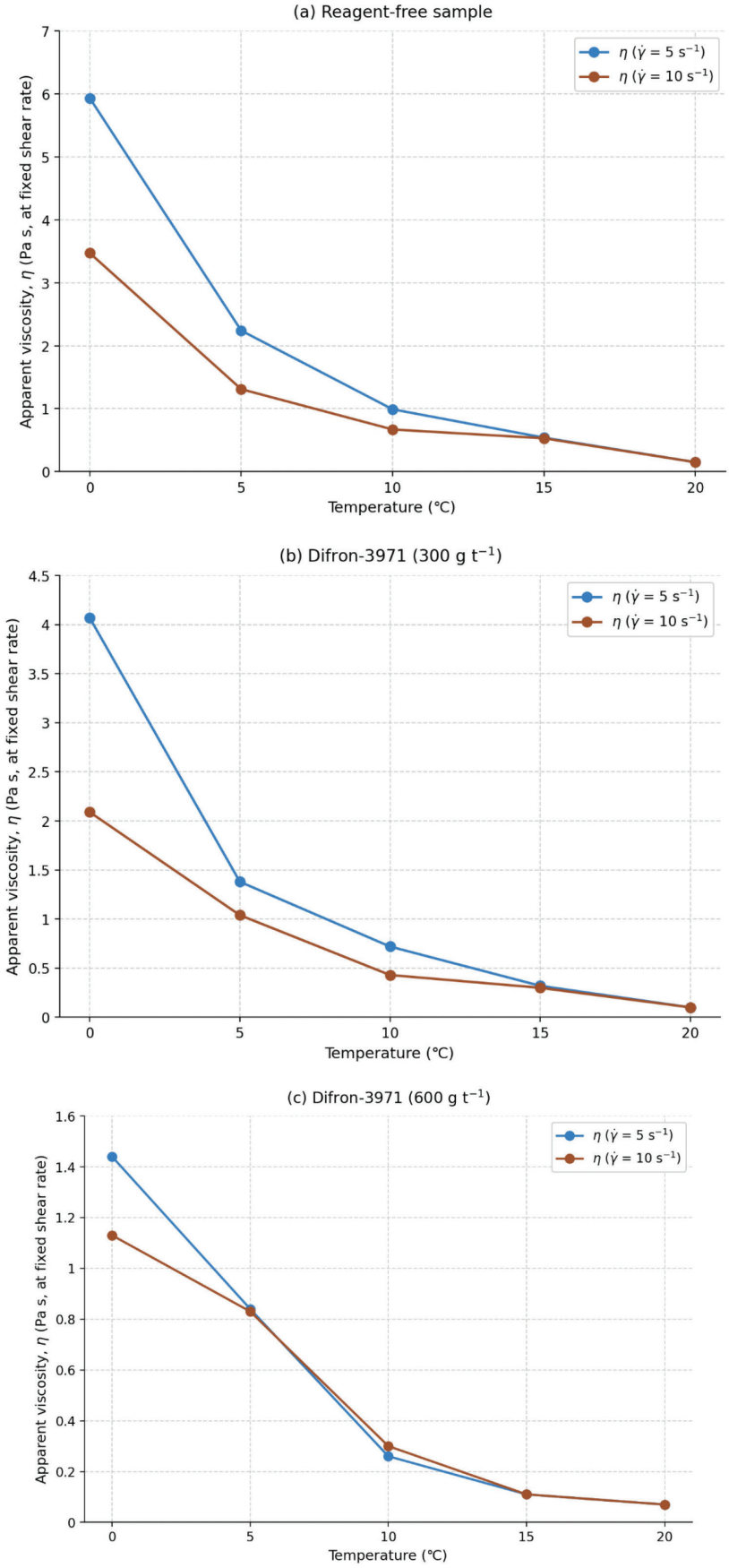

Fig. 4 – *Temperature dependence of apparent viscosity (η) of high-paraffin crude oil at fixed shear rates ($\dot{\gamma}$ = 5 s^{-1} and $\dot{\gamma}$ = 10 s^{-1}) under different reagent conditions: (a) reagent-free sample; (b) Difron-3971 (300 g t^{-1}); (c) Difron-3971 (600 g t^{-1}); (d) HY-154 (300 g t^{-1}); (e) HY-154 (600 g t^{-1}); (f) DHC (600 g t^{-1})*

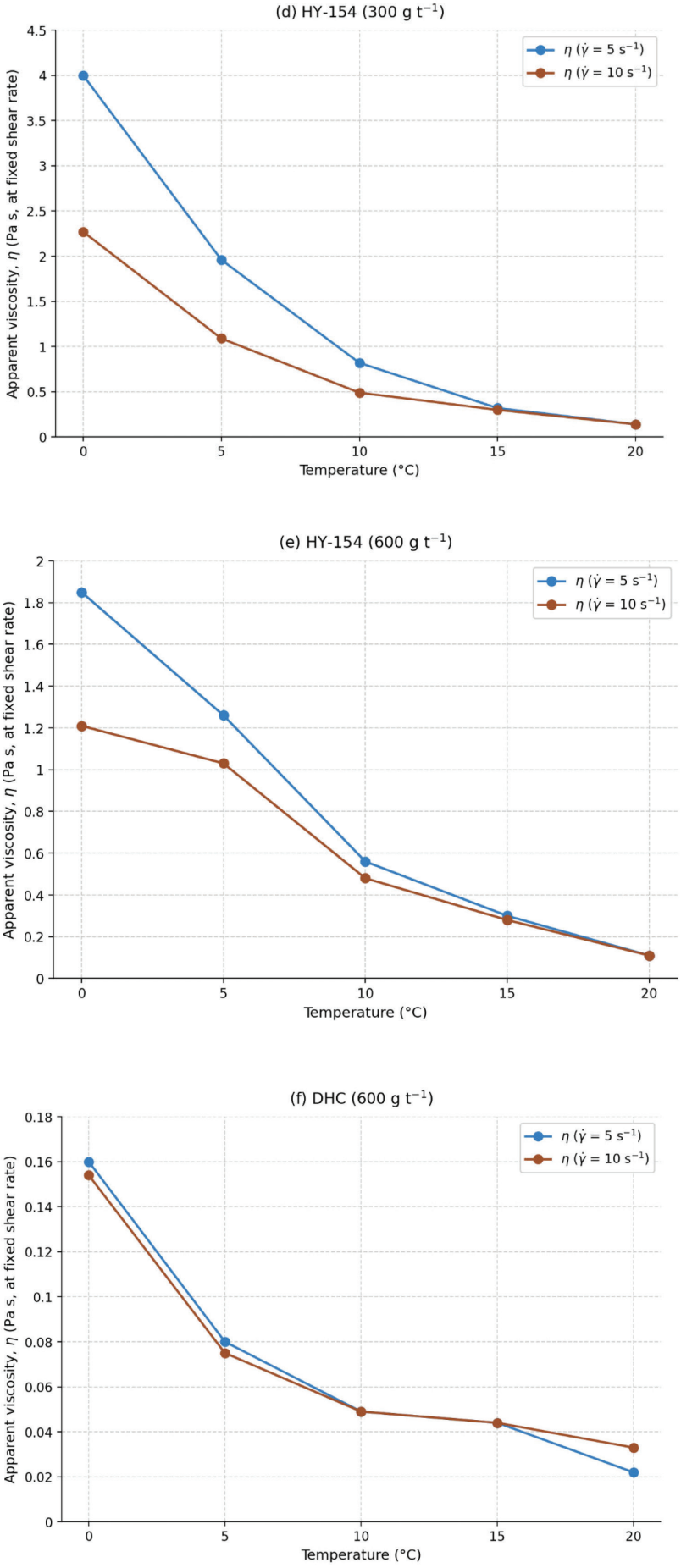

Fig. 4 – *continued*

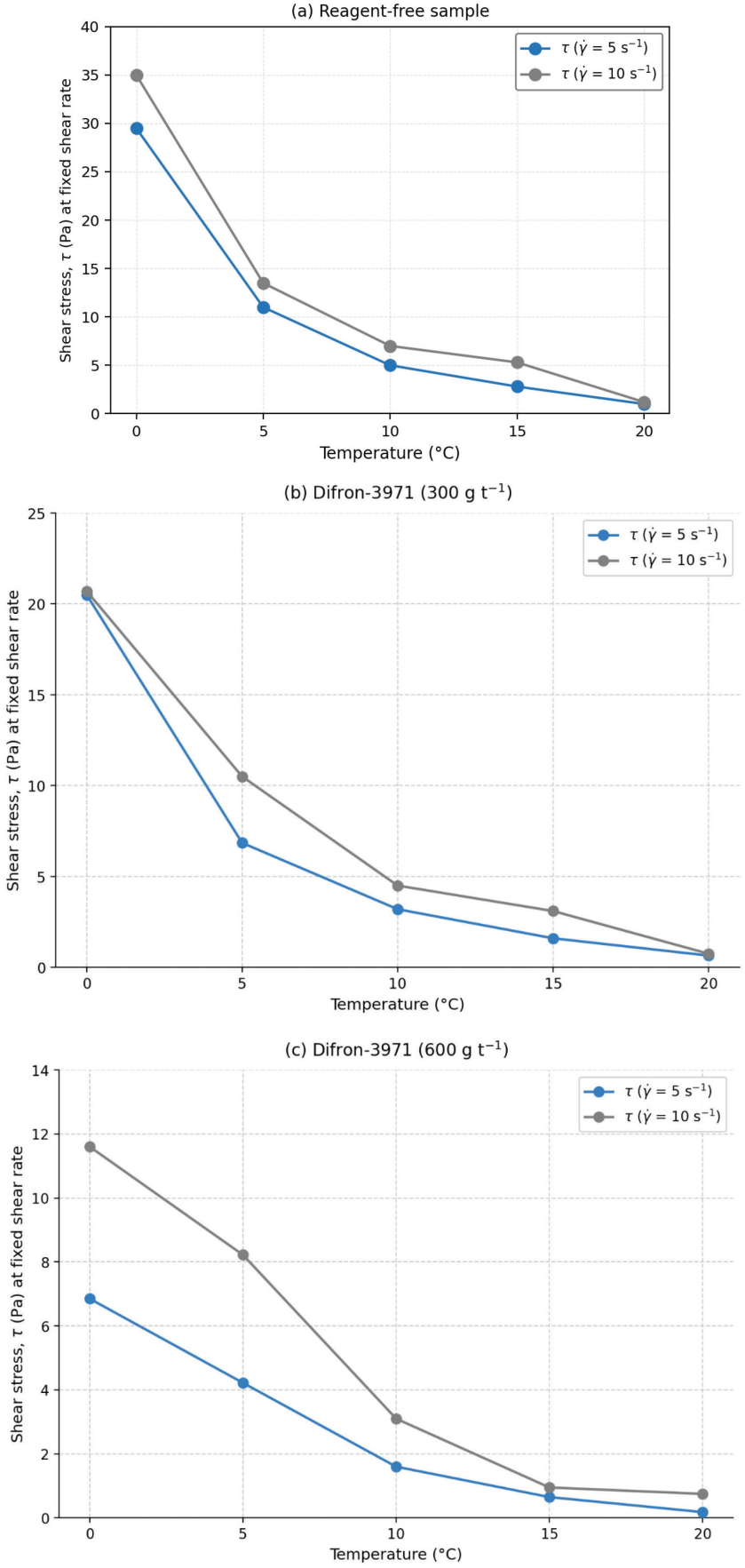

Fig. 5 – *Temperature dependence of shear stress (τ) of high-paraffin crude oil at fixed shear rates ($\dot{\gamma}$ = 5 s^{-1} and $\dot{\gamma}$ = 10 s^{-1}) under different reagent conditions: (a) reagent-free sample; (b) Difron-3971 (300 g t^{-1}); (c) Difron-3971 (600 g t^{-1}); (d) HY-154 (300 g t^{-1}); (e) HY-154 (600 g t^{-1}); (f) DHC (600 g t^{-1})*

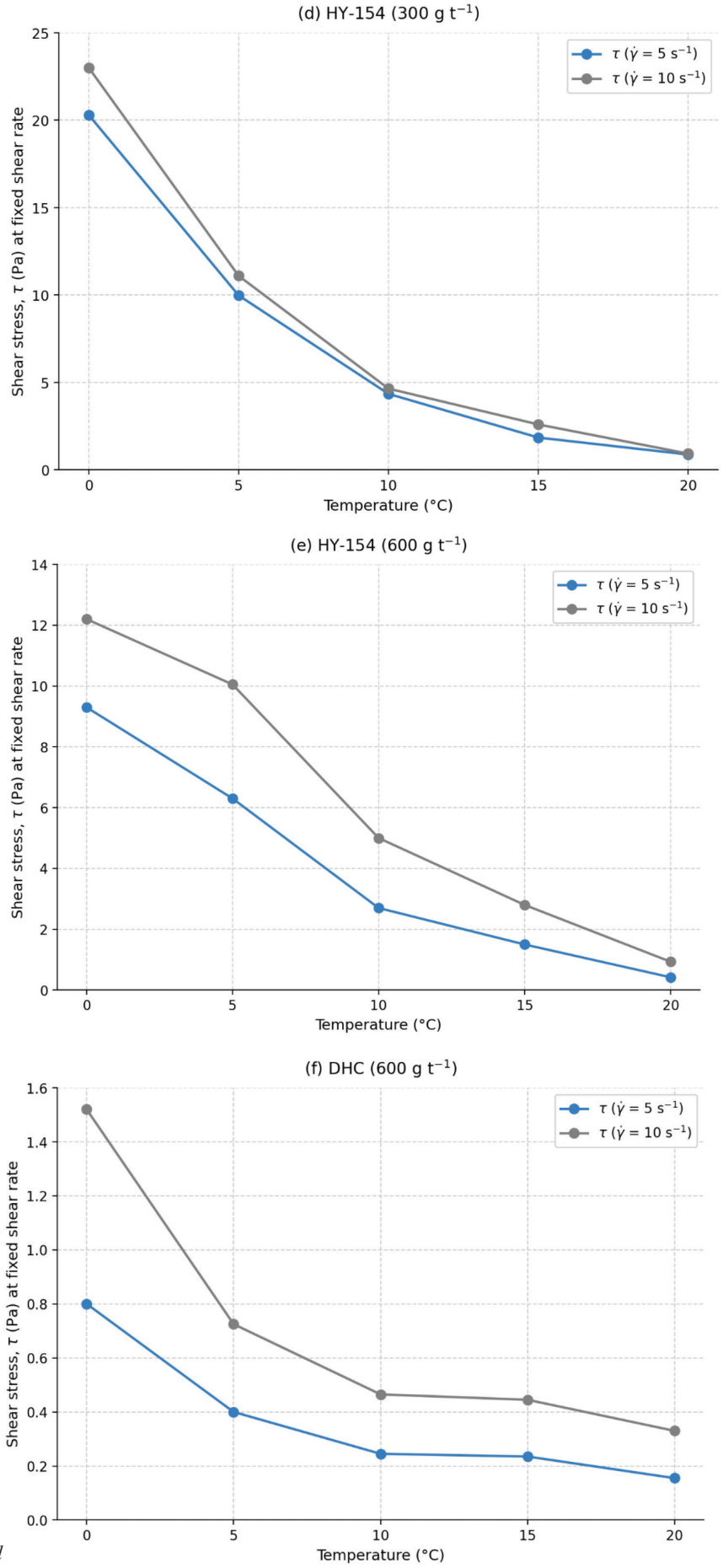

Fig. 5 – *continued*

mensional network within the oil. Such a network imparts solid-like characteristics to the system, meaning that a finite stress must be applied to initiate flow. Accordingly, the rapid growth of τ_0 at low temperatures reflected a transition from a viscous liquid to a more structured, gel-like state.

The reagent-free oil exhibited the highest yield stress values over the entire temperature range, indicating the strongest degree of structural reinforcement. In contrast, the presence of chemical reagents significantly suppressed the increase in yield stress, demonstrating their ability to interfere with paraffin crystal aggregation and to weaken interactions between crystals. Among the tested chemical reagents, the DHC composite provided the most pronounced reduction in τ_0, indicating effective modification of the crystallization process and enhanced disruption of the internal structural framework.

The results shown in Fig. 3 clearly demonstrate the decisive roles of both temperature and chemical treatment in controlling yield stress and, consequently, flow initiation in high-paraffin oil systems. These findings provide a solid basis for the subsequent analysis of plastic viscosity, apparent viscosity, and the flow behavior index.

The next stage of the study investigates the temperature-dependent variation of viscosity at fixed shear rates for high-paraffin oils under different reagent conditions. The combined effects of thermal conditions and chemical additives on the internal structural organization of the system are presented in Fig. 4.

The results presented in Fig. 4 indicate that temperature played a dominant role in controlling the viscosity of high-paraffin oils, regardless of shear rate or the presence of chemical reagents. In the reagent-free sample, the high viscosity observed at low temperatures reflected the formation of a well-developed paraffin crystal network that strongly restricts flow. As temperature increased, partial melting and progressive breakdown of this network occured, resulting in a pronounced reduction in viscosity.

At both investigated shear rates, the apparent viscosity measured at $\dot{\gamma} = 5\ s^{-1}$ remained consistently higher than that at $\dot{\gamma} = 10\ s^{-1}$, confirming thixotropic behavior characteristic of non-Newtonian fluids. However, this difference gradually diminished at higher temperatures, indicating weakening of the internal structure and a progressive transition toward more Newtonian-like flow behavior.

The addition of chemical reagents led to a noticeable reduction in apparent viscosity over the entire temperature range. Among the tested additives, the DHC composite exhibited the strongest viscosity-reducing effect, indicating effective disruption of interactions between crystals and suppression of paraffin structure formation. Difron-3971 and HY-154 also contributed to viscosity reduction, particularly at higher dosages.

The obtained results support the applicability of the Herschel–Bulkley model for describing the rheological behavior of high-paraffin oils.

To further elucidate the flow characteristics, the temperature dependence of shear stress at different shear rates was analyzed. Accordingly, the investigated high-paraffin blended crude oil was examined under reagent-free conditions and in the presence of various chemical additives, and the corresponding results are presented in Fig. 5.

As illustrated in the figure, temperature exerted a strong influence on the shear stress behavior of the high-paraffin blended crude oil under all investigated conditions. In the reagent-free system, the relatively high shear stress values observed at low temperatures—particularly at lower shear rates—indicated the presence of a rigid paraffin crystal network that provided significant resistance to deformation.

The application of chemical reagents resulted in a pronounced reduction in shear stress across the entire temperature range. In particular, the DHC composite exhibited the lowest shear stress values, indicating the most effective suppression of structure formation and a corresponding improvement in flowability. The effects of Difron-3971 and HY-154 on shear stress became more pronounced with increasing dosage and demonstrated high efficiency; however, the DHC composite consistently showed superior performance compared to both individual depressor additives.

The combined influence of temperature and chemical additives clearly confirms their significant contribution to inhibiting solid paraffin structure formation. The observed rheological behavior further supports the applicability of the Bingham and Herschel–Bulkley models for describing the flow behavior of high-paraffin oils.

Fig. 6 presents the results of plastic viscosity (K_p) measurements of the high-paraffin blended crude oil at different temperatures for both reagent-free and reagent-treated samples, clearly indicating a gradual weakening of the internal structure with increasing temperature.

As observed in Fig. 6, for all investigated systems, the plastic viscosity (K_p) decreased steadily with increasing temperature, confirming that thermal effects contributed to the breakdown of the paraffin crystal network.

The application of chemical reagents led to a significant reduction in plastic viscosity across the entire temperature range. This effect was most pro-

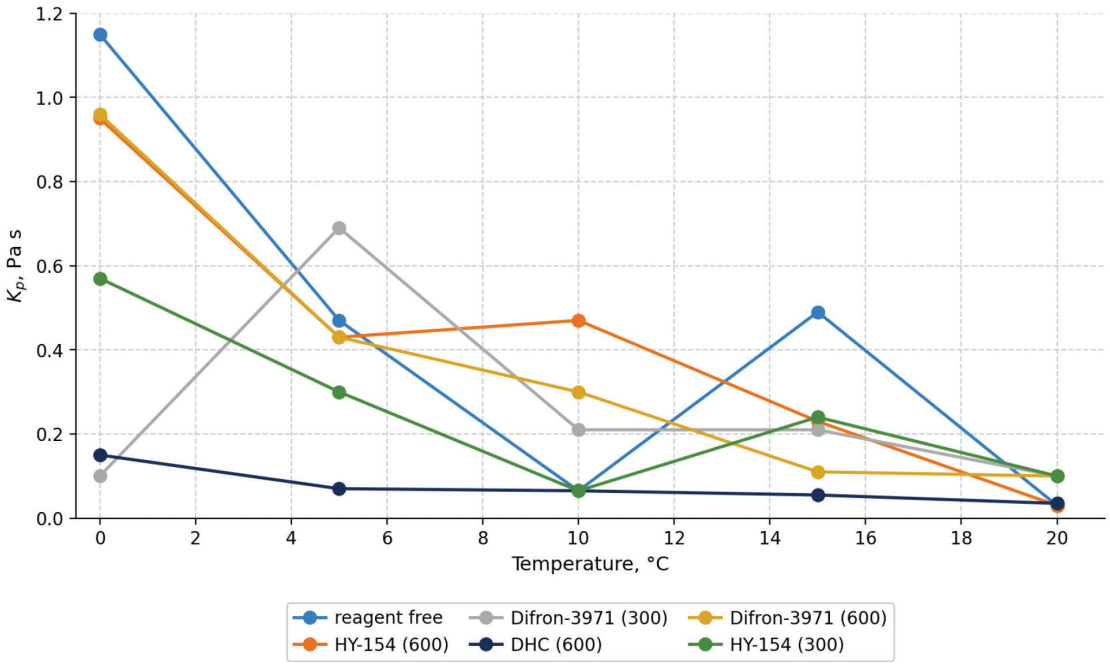

Fig. 6 – *Effect of temperature on plastic viscosity (K_p) of high-paraffin crude oil for reagent-free samples and samples treated with Difron-3971, HY-154, and DHC at different dosages*

nounced for the DHC composite, which exhibited the lowest K_p values, indicating effective disruption of interactions between crystals and suppression of structure formation.

Nevertheless, one of the most critical challenges associated with high-paraffin oils is their tendency to exhibit solidification behavior even at relatively elevated temperatures, resulting in complete flow stoppage. In this context, the relationship between cooling rate and both the pour point temperature and kinematic viscosity of the high-paraffin oil was investigated. The results of this analysis are presented as graphical dependencies in Fig. 7.

Fig. 7 illustrates how the viscosity and pour point of the investigated high-paraffin oil sample varied solely as a function of cooling rate, in the

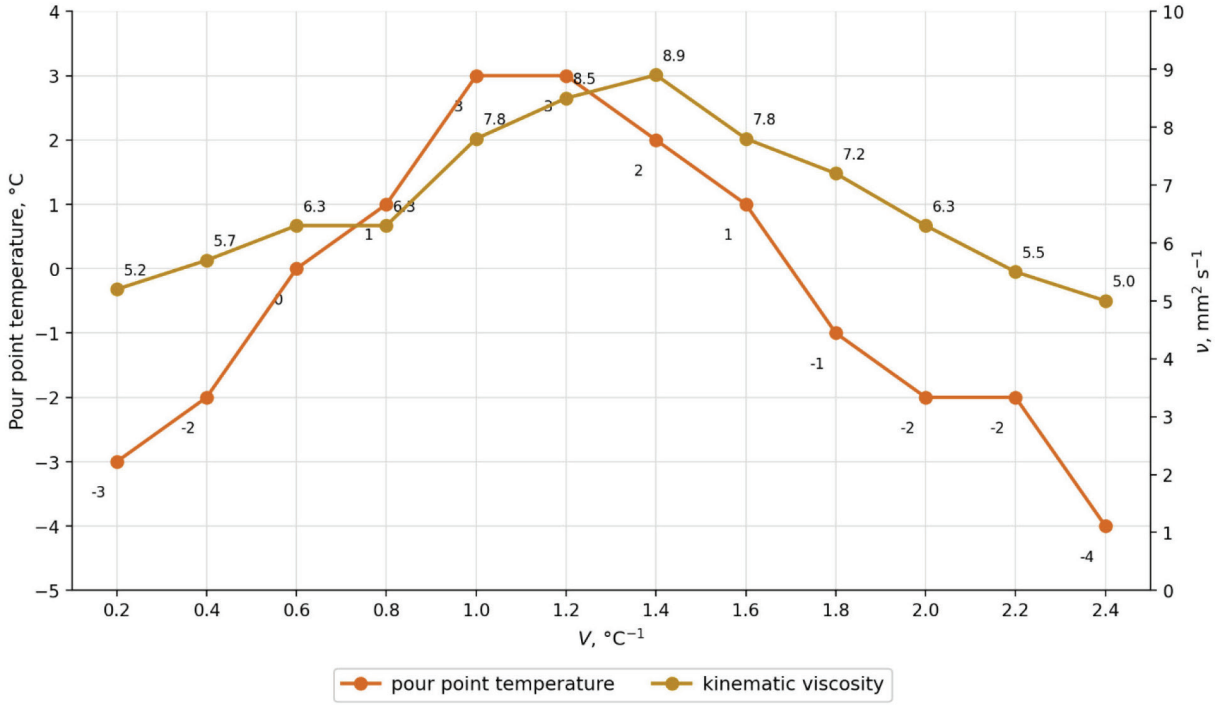

Fig. 7 – *Relationship between cooling rate (V, °C min^{-1}), pour point temperature, and kinematic viscosity of high-paraffin crude oil*

absence of any chemical additives. The obtained results demonstrate that the cooling rate exerted a decisive influence on the low-temperature behavior of high-paraffin oils. At lower cooling rates, a pronounced increase in kinematic viscosity was observed together with an elevation of the pour point temperature. This behavior can be explained by intensive growth and aggregation of paraffin crystals, which promoted the formation of a well-developed and mechanically stable crystalline network within the oil.

When the cooling rate exceeded a certain optimal range, both the pour point temperature and the kinematic viscosity decreased. Under rapid cooling conditions, the time available for paraffin crystal growth, alignment, and interconnection is limited, leading to the formation of a finer and less interconnected crystal structure. As a result, flow resistance reduced and low-temperature flowability improved.

The non-monotonic behavior observed for both pour point temperature and kinematic viscosity indicated the existence of an optimal cooling rate at which the balance between crystal nucleation and growth provided the strongest structural reinforcement. These findings highlight the close relationship between thermal history and rheological response and indicate that the pour point temperature can serve as an effective indirect indicator of structural rigidity and flow resistance in high-paraffin oil systems.

To further evaluate the adequacy of the rheological description of the investigated oil, a comparative fitting analysis was performed using the Herschel–Bulkley, Bingham, and Power-law models. The corresponding correlation coefficients and goodness-of-fit parameters for these models are summarized in Table 4.

Table 4 provides a comparative assessment of the fitting performance of three rheological models applied to describe the flow behavior of the investigated crude oil. The results clearly show that the Herschel–Bulkley model offered the best agreement with the experimental data, exhibiting the highest correlation coefficient (R^2 = 0.995). This indicates that the model was capable of capturing the essential rheological features of the system, particularly the presence of a yield stress (τ_0) and the nonlinear dependence of viscosity on shear rate.

The Bingham model demonstrated a moderate level of agreement with the experimental results (R^2 = 0.980). While this model accounted for the existence of a yield stress, its ability to describe shear-rate-dependent viscosity was limited. Consequently, the Bingham model did not fully reflect the complex rheological behavior of crude oil systems that exhibited pronounced structural organization and shear-thinning characteristics.

Among the three models, the Power-law model showed the lowest degree of agreement with the experimental data (R^2 = 0.950). This reduced performance can be attributed to the absence of a yield stress term in the model formulation. As a result, the Power-law model was less suitable for describing the structural development of crude oil at low temperatures and its resistance to flow initiation.

The results summarized in Table 4 confirm that the Herschel–Bulkley model, which simultaneously incorporated yield stress and shear-thinning behavior, provided the most appropriate framework for

Table 4 – *Comparative analysis of the goodness-of-fit indicators of different rheological models for crude oil (temperature range: 0–20 °C, reagent-free sample)*

Model	Parameters	R^2	Remark
Herschel–Bulkley	τ_0, K, n	0.995	Best fit
Bingham	τ_0, K_p	0.980	Moderate fit
Power-law	K, n	0.950	Yield stress not considered

Table 5 – *Temperature dependence of the flow behavior index (n) under the effect of different reagents and compositions*

System / Additive	Dosage, g t^{-1}	n (20 °C)	n (10 °C)	n (0 °C)	Remark
Reagent-free	–	0.55	0.50	0.45	Very strong shear-thinning
Difron-3971	300	0.69	0.63	0.60	Strong shear-thinning
Difron-3971	600	0.73	0.67	0.63	Strong shear-thinning
HY-154	300	0.75	0.70	0.68	Moderate shear-thinning
HY-154	600	0.78	0.72	0.70	Moderate shear-thinning
DHC composite	600	0.92	0.88	0.85	Nearly Newtonian

modeling the rheological properties of the studied crude oil.

To further characterize the rheological response of the crude oil dispersion system under reagent-free conditions, as well as in the presence of individual reagents and the composite formulation, the temperature dependence of the flow behavior index (n) was analyzed. The corresponding values of the flow behavior index for the untreated oil, reagent-treated samples, and the composite at different temperatures are presented in Table 5.

Table 5 presents a comparative analysis of the temperature-dependent variation of the flow behavior index for crude oil under reagent-free conditions, in the presence of individual reagents, and after treatment with the composite formulation. For the reagent-free crude oil, flow behavior index values below 0.5 across the entire temperature range indicated a very strong shear-thinning character and pronounced non-Newtonian behavior of the dispersion system. As temperature decreased, the flow behavior index further declined, reflecting an increase in structural organization within the oil and a corresponding rise in internal resistance during flow.

When the Difron-3971 reagent was applied, the flow behavior index showed a clear dependence on both temperature and reagent dosage. This effect can be attributed to the weakening of ARPD-related interactions and partial suppression of structure formation. However, since the flow behavior index remained below 0.7, the system still exhibited strong shear-thinning behavior, indicating that structural elements were reduced but not completely eliminated.

In the case of the HY-154 reagent, higher values of the flow behavior index were obtained, and no sharp decrease wass observed even at lower temperatures. This suggested that HY-154 not only destabilized structural aggregates within the crude oil system but also contributed to a more stable rheological response. Overall, the results indicated that HY-154 induced a moderate shear-thinning behavior and improved flow stability over the investigated temperature range.

At the maximum dosage of the DHC composite, the flow behavior index varied between 0.85 and 0.92, depending on temperature, indicating that the crude oil system approached near Newtonian flow behavior. The composite effectively inhibited structural organization, limited the formation of gel-like networks, and significantly weakened the ability of ARPD aggregates to form stable structures.

The flow behavior index serves as a quantitative indicator of the influence of chemical reagents and composite formulations on the degree of structural organization in crude oil systems. An increase in the flow behavior index reflects a reduction in non-Newtonian effects and improved flow stability, which is particularly important for facilitating crude oil transportation under low-temperature conditions.

In addition, the variation in the relationship between shear stress and shear rate during upward and downward shear sweeps is presented in Fig. 8. These curves enable a comparative evaluation of the rheological behavior of the crude oil under reagent-free conditions and after treatment with the composite at a dosage of 600 g t^{-1}, with particular emphasis on structure formation under shear and subsequent structural recovery. This approach, often referred to in the literature as the "golden triangle," characterizes low-temperature crude oil flow behavior and provides a mechanistic interpretation of the interrelationship among key rheological parameters, namely pour point, yield stress (τ_0), and effective viscosity. The upward and downward shear stress curves obtained at different shear rates demonstrate that these parameters vary in a correlated manner and are directly governed by the degree of structural organization within the system. Within the framework of the "golden triangle" concept, the presented results visually and quantitatively confirm the structure-weakening effect of the composite and the resulting improvement in low-temperature crude oil flowability.

Fig. 8 illustrates the dependence of shear stress on shear rate during both increasing (τ-up) and decreasing (τ-down) shear conditions. The observed deviation between the upward and downward flow curves indicated the presence of rheological hysteresis, which reflects time-dependent structural rearrangement processes within the crude oil dispersion system.

During the increase in shear rate, partial disruption of paraffin–asphaltene–resin aggregates occurred, whereas upon decreasing shear rate the structure did not fully recover within the experimental time scale. This behavior indicated structural sensitivity of the system to mechanical loading and confirmed the non-Newtonian character of the studied crude oil.

Fig. 8a demonstrates a noticeable separation between the τ-up and τ-down curves, indicating the presence of a hysteresis loop associated with time-dependent structural rearrangement of the paraffin–resin–asphaltene network. As shear rate increases, structural aggregates were progressively disrupted and partially oriented along the flow direction. When the shear rate decreased, the initial structure was not fully restored immediately, resulting in lower shear stress values along the τ-down curve. This behavior indicated the presence of structural relaxation processes typical for paraffin-containing dispersed systems and suggested limited structural reversibility within the experimental timeframe.

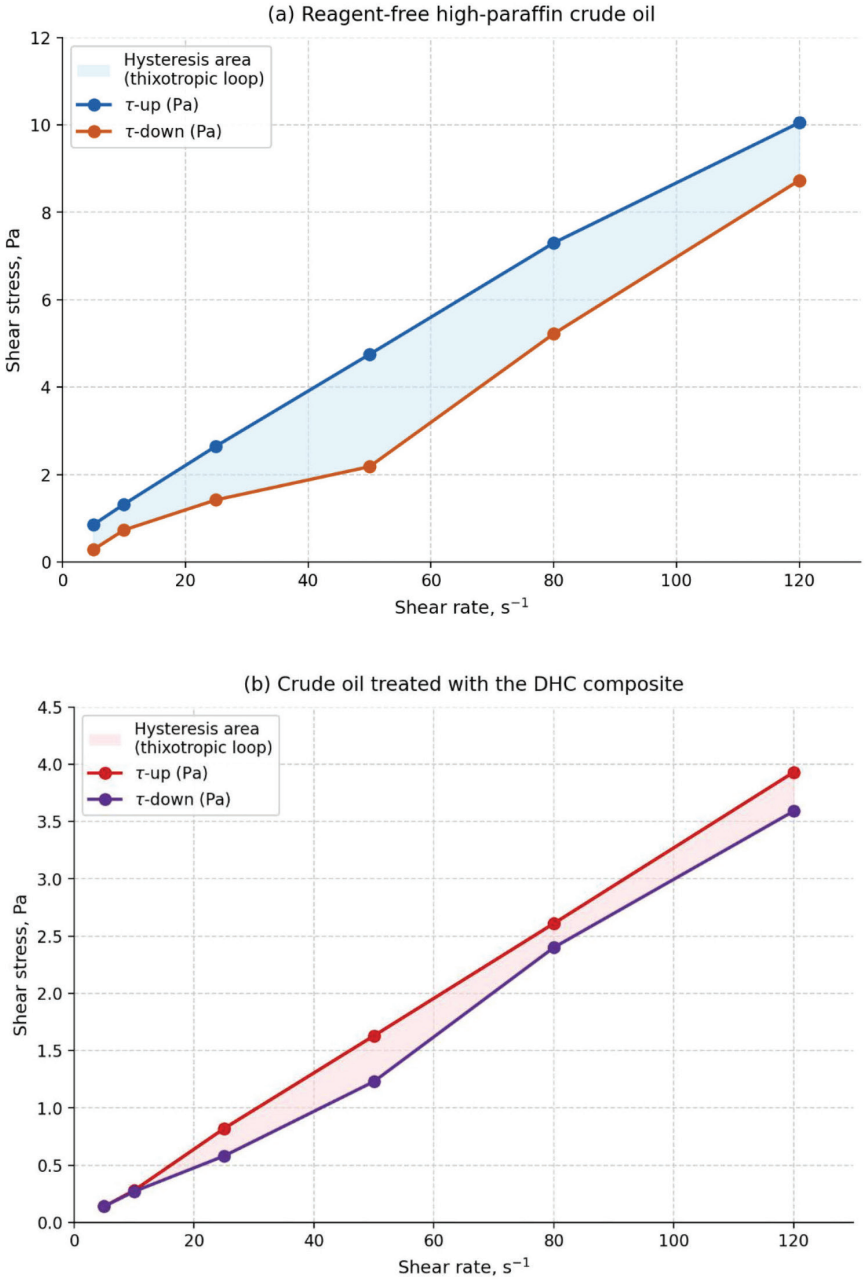

Fig. 8 – *Shear stress versus shear rate curves illustrating hysteresis behavior for: (a) reagent-free high-paraffin crude oil; (b) crude oil treated with the DHC composite*

The presence of hysteresis indicated that the rheological response of the crude oil was influenced not only by instantaneous shear conditions but also by the previous deformation history. Such behavior is commonly associated with structured dispersions containing wax crystals and asphaltene aggregates, where intermolecular interactions and crystal networking govern resistance to deformation.

In contrast, Fig. 8b shows a significantly smaller difference between τ-up and τ-down curves after treatment with the composite additive. The reduced hysteresis loop indicates weakening of intermolecular interactions and partial disruption of the paraffin–resin–asphaltene network structure. As a result, structural rearrangement occurred more rapidly and resistance to deformation decreased, leading to improved flow behavior. The reduced hysteresis suggests that the composite additive limited formation of stable structural networks and promoted a more homogeneous dispersion state.

The decrease in hysteresis area after treatment indicates suppression of structure-forming interactions responsible for increased flow resistance at low temperatures, confirming the effectiveness of the composite additive in modifying the rheological behavior of the crude oil system.

Rheological parameters obtained using the Herschel–Bulkley model made it possible to evaluate the degree of structural organization, the formation of gel-like networks, and the influence of temperature on these structures. From this perspective, examining correlations between the pour point and the parameters τ_0 and K, offered deeper insight into the mechanisms governing low-temperature flow behavior. The presence of clear and strong linear relationships between the pour point and both yield stress (τ_0) and consistency index (K) is illustrated in Fig. 9. Rheological parameters obtained using the Herschel–Bulkley model provide insight into the structural organization of highly paraffinic crude oil systems, including the formation of gel-like networks and the temperature sensitivity of these structures. In this context, correlations between pour point and the rheological parameters yield stress (τ_0) and consistency index (K) allowed deeper interpretation of low-temperature flow behavior.

As illustrated in Fig. 9, strong linear relationships exist between pour point, yield stress, and consistency index, forming a characteristic "golden triangle" of low-temperature rheology. This relationship reflects the coupled evolution of crystallization temperature, structural strength, and resistance to flow, which together control the transportability of paraffin-rich crude oils under cooling conditions.

The first graph (Fig. 9a) demonstrates a strong proportional relationship between yield stress (τ_0) and pour point, with a high correlation coefficient (R^2 = 0.9389). The increase in pour point corresponds to higher resistance required to initiate flow, indicating progressive strengthening of the internal structure. This behavior is associated with intensified paraffin crystallization and enhanced interaction between asphaltene–resin components, leading to formation of a mechanically stable spatial network.

The second graph (Fig. 9b) shows a strong linear correlation between the consistency index (K) and pour point (R^2 = 0.986). Higher pour point values correspond to increased effective viscosity and stronger resistance to deformation. This trend confirms that structural aggregates formed at lower temperatures exhibit pronounced gel-like behavior, increasing the energy required to sustain flow.

The third graph (Fig. 9c) presents a strong positive relationship between consistency index (K) and yield stress (τ_0), characterized by R^2 = 0.9651. The close agreement between these parameters indicates that both describe the same structural transformation process associated with paraffin crystal network development. Their simultaneous increase confirms that rheological resistance and structural strength evolve together as temperature decreases.

Taken together, these relationships form the so-called golden triangle of low-temperature rheology, linking crystallization behavior (pour point) with mechanical strength (yield stress) and flow resistance (consistency index). The triangular correlation confirms that the deterioration of flow properties in highly paraffinic oils is governed by a unified structural mechanism involving progressive formation of interconnected paraffin–resin–asphaltene networks.

The high correlation coefficients (R^2 = 0.94–0.99) indicate strong consistency between rheological parameters derived from the Herschel–Bulkley model. Such agreement is expected for paraffin-containing crude oils, where crystallization processes simultaneously influence yield stress and viscosity-related parameters.

The results demonstrate that the pour point is a key parameter controlling the rheological behavior of crude oil at low temperatures. An increase in pour point leads to a proportional rise in both yield stress and consistency index, reflecting enhanced structural organization and reduced flowability. These correlations provide a reliable basis for evaluating the effectiveness of chemical reagents and composite formulations designed to improve the low-temperature flow properties of crude oil.

The superior performance of the DHC composite relative to the individual depressor additives Difron-3971 and HY-154 can be attributed to the synergistic interaction between its constituent components and their combined effect on the paraffin crystallization process.

Difron-3971 is a polymeric depressor additive whose active molecules contain alkyl side chains capable of co-crystallizing with paraffin wax. By incorporating into the growing paraffin crystal lattice, Difron-3971 disrupts the regular crystal structure, reduces the size of paraffin crystals, and inhibits their aggregation into three-dimensional networks. This mechanism lowers both the pour point and yield stress of the crude oil system.

HY-154 is a nitrogen-containing dispersant with a high total base number (TBN = 15–30 mg KOH/g), which imparts surface-active properties to the additive. Its polar nitrogen-containing functional groups adsorb onto the surface of paraffin crystals and asphaltene aggregates, forming a steric barrier that prevents crystal–crystal interactions and inhibits the growth of the paraffin–resin–asphaltene network. This mechanism is complementary to that of Difron-3971 and contributes to the stabilization of the dispersion system at low temperatures.

The solvent components of the DHC formulation — kerosene (55 wt.%) and xylene (14 wt.%) — serve a dual function. Firstly, they ensure uniform distribution and enhanced penetration of the active components into the crude oil matrix. Secondly, aromatic solvents such as xylene are known to

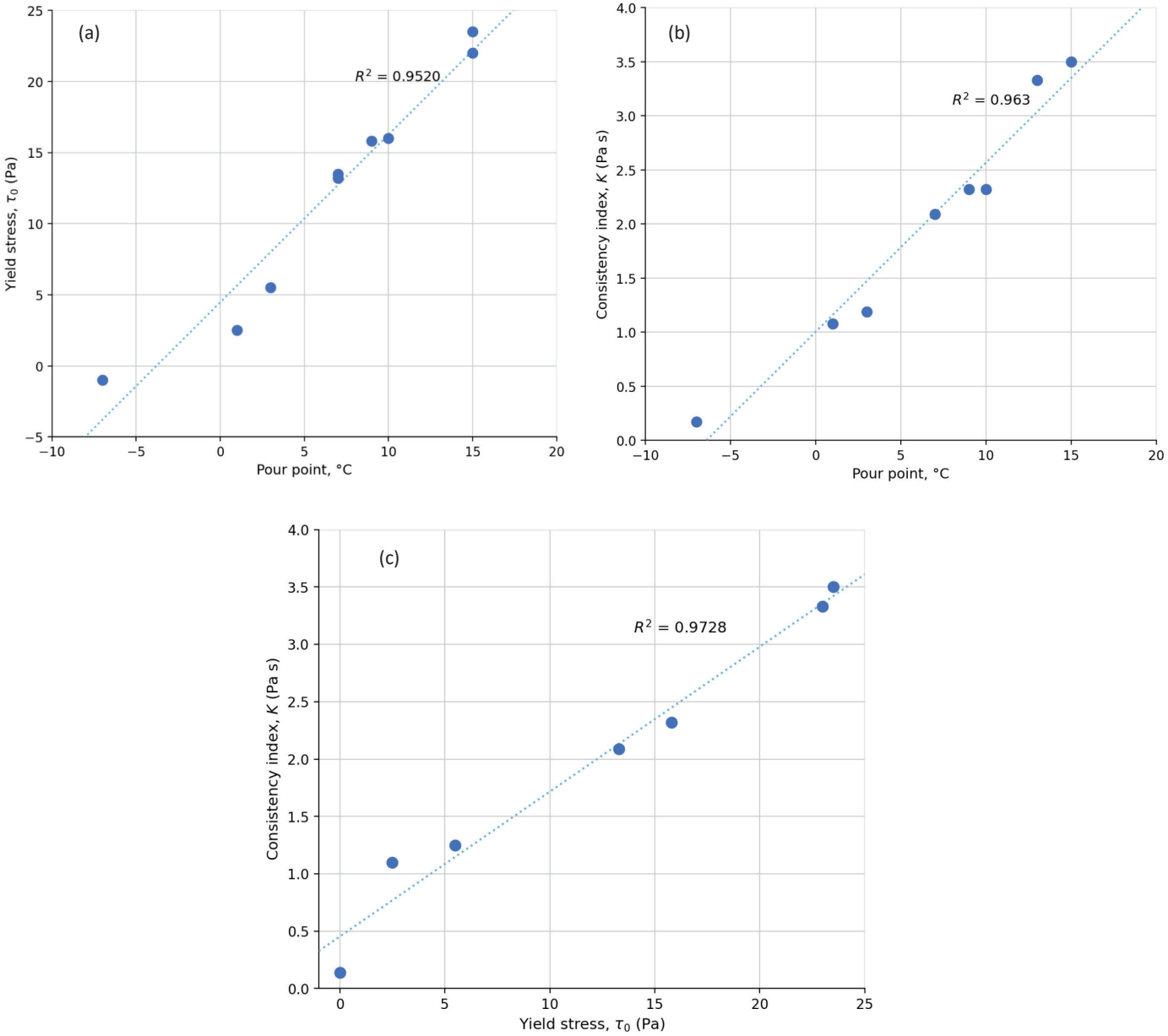

Fig. 9 – *Golden triangle relationship between pour point, yield stress (τ_0), and consistency index (K) for highly paraffinic crude oil, illustrating the coupled evolution of crystallization temperature, structural strength, and flow resistance*

disperse asphaltene aggregates and reduce their tendency to associate with paraffin crystals, thereby further weakening the internal structural network.

The synergistic combination of these mechanisms — crystal lattice disruption by Difron-3971, steric stabilization by HY-154, and asphaltene dispersion by the aromatic solvent — results in a more comprehensive and effective suppression of structure formation compared to either additive applied individually. Consequently, the DHC composite achieves a substantially higher flow behavior index (n = 0.85–0.92), lower yield stress, and reduced wax deposition tendency, confirming its superior efficiency in improving the low-temperature transportability of high-paraffin crude oils.

Conclusions

Comprehensive quantitative rheological analysis unequivocally demonstrates the dominant role of temperature in governing structural strength and flow behavior in high-paraffin oil systems. A pronounced increase in yield stress (τ_0), apparent viscosity, and plastic viscosity was observed with decreasing temperature, while the flow behavior index (n) declined to values below 0.5 for the reagent-free system, indicating extreme shear-thinning and strongly non-Newtonian behavior. The strong statistical correlations established between pour point temperature and key rheological parameters (R^2 up to 0.94 for τ_0 and 0.99 for the consistency index K)

confirm that pour point serves as a reliable indirect indicator of internal structural rigidity and resistance to flow at low temperatures.

Model comparison clearly establishes the Herschel–Bulkley formulation as the most physically and statistically appropriate framework for describing the rheological behavior of high-paraffin oils. The superior agreement between experimental and modelled data (R^2 = 0.995), relative to the Bingham (R^2 = 0.980) and Power-law (R^2 = 0.950) models, highlights the necessity of simultaneously accounting for both yield stress and nonlinear shear dependence. This finding is particularly critical for accurately capturing flow initiation and structural breakdown phenomena under low-temperature transport conditions.

Chemical modification was shown to be highly effective in mitigating structure formation and improving low-temperature flow performance. Application of the DHC composite resulted in a substantial increase in the flow behavior index (n = 0.85–0.92), reflecting a clear transition toward near-Newtonian flow, accompanied by significant reductions in yield stress and rheological hysteresis. Independent confirmation from deposit mass measurements and shear stress–shear rate hysteresis analyses demonstrates that chemical treatment suppresses paraffin-induced network formation, weakens gel-like structures, and markedly reduces resistance to flow initiation. Collectively, these results confirm that composite chemical formulations represent a robust and efficient strategy for enhancing the transportability and operational reliability of high-paraffin oil systems under low-temperature conditions.

References

1. *Sulaiman, I. N., Zeinalabideen, M. J., Abed, A. A.,* An improved correlation to investigate the effect of chemical additives on the mobility ratio of two-phase flow, Period. Eng. Nat. Sci. **9** (2021) 227. doi: https://doi.org/10.21533/pen.v9.i1.726
2. *Ali, M. F., Alqam, M. H.,* The role of asphaltenes, resins and other solids in the stabilization of water in oil emulsions and its effects on oil production in Saudi oil fields, Fuel **79** (2000) 1309. doi: https://doi.org/10.1016/S0016-2361(99)00240-0
3. *Alnaimat, F., Al-Sarkhi, A.,* Wax deposition and prediction in petroleum pipelines, J. Pet. Sci. Eng. **193** (2020) 107408. doi: https://doi.org/10.1016/j.petrol.2020.107408
4. *Bakhtizin, R. N., Karimov, R. M., Mastobayev, B. N.,* Impact of macromolecular components on rheological properties depending on the structural-group and fractional composition of oil, SOCAR Proc. **1** (2016) 42. doi: https://doi.org/10.5510/OGP20160100269
5. *Wu, B., Li, Y., Li, X., Zhu, J., Ma, R., Hu, S.,* Organochlorine compounds with a low boiling point in desalted crude oil: Identification and conversion, Energy Fuels **32** (2018) 6475. doi: https://doi.org/10.1021/acs.energyfuels.8b00205
6. *Gasimzade, A. V.,* Study of multifunctional compositions in the preparation and transportation of heavy oils, Vopr. Khim. Khim. Tekhnol. **4** (2024) 25. doi: https://doi.org/10.32434/0321-4095-2024-155-4-25-33
7. *Rogel, E., Lezcano, M., Yee, N., Witt, M.,* Effect of aging on deposit characteristics obtained by crude oil blending, Energy Fuels **37** (2023) 1848. doi: https://doi.org/10.1021/acs.energyfuels.2c03511
8. *Liu, G., Xu, X., Gao, J.,* Study on the compatibility of high-paraffin crude oil with electric desalting demulsifiers, Energy Fuels **17** (2003) 625. doi: https://doi.org/10.1021/ef020166g
9. *Abdullah, M. M. S., Al-Lohedan, H. A.,* Demulsification of Arabian heavy crude oil emulsions using novel amphiphilic ionic liquids based on glycidyl 4-nonylphenyl ether, Energy Fuels **33** (2019) 12916. doi: https://doi.org/10.1021/acs.energyfuels.9b03148
10. *Jennings, D. W., Weispfenning, K.,* Effect of shear and temperature on wax deposition: Cold finger investigation with a Gulf of Mexico crude oil, Energy Fuels **19** (2005) 1376. doi: https://doi.org/10.1021/ef0497346
11. *Rogel, E., Ovalles, C., Vien, J., Moir, M.,* Asphaltene characterization of paraffinic crude oils, Fuel **178** (2016) 71. doi: https://doi.org/10.1016/j.fuel.2016.03.030
12. *Atta, A. M., Fadda, A. A., Abdel-Rahman, A. A.-H., Ismail, H. S., Fouad, R. R.,* Application of new modified poly(ethylene oxide)-block-poly(propylene oxide)-block-poly(ethylene oxide) copolymers as demulsifier for petroleum crude oil emulsion, J. Dispersion Sci. Technol. **33** (2012) 775. doi: https://doi.org/10.1080/01932691.2011.584484
13. *Bai, Z. S., Wang, H. L.,* Crude oil desalting using hydrocyclones, Chem. Eng. Res. Des. **85** (2007) 1586. doi: https://doi.org/10.1016/S0263-8762(07)73203-3
14. *Mingalev, P. G., Grishaev, P. A., Erlikh, G. V., Lisichkin, G. V.,* Magnetic sorption deasphalting of oil fractions, Chem. Chem. Technol. **11** (2022) 76. doi: https://doi.org/10.6060/ivkkt.20226511.6700
15. *Al-Sayyab, A. K. S., Abdulwahid, M. A.,* Using injected additive materials to improve pipeline transportation in real-world experiments and computational fluid dynamics, J. Therm. Eng. **10** (2024) 826. doi: https://doi.org/10.14744/thermal.0000834
16. *Nurullayev, V. H., Murvatov, F. T., Gasimzade, A. V.,* On the issues of perspective for the development of the Siyazan monoclinal oil field of the Republic of Azerbaijan, SOCAR Proc. **1** (2022) 84. doi: https://doi.org/10.5510/OGP2022SI100649
17. *Yamini, K., Kishore, P. S., Raju, V. D.,* Effect of diethyl ether and isobutanol as fuel additives on the diesel engine attributes fueled with subabul seed biodiesel, J. Therm. Eng. **11** (2025) 215. doi: https://doi.org/10.14744/thermal.0000914
18. *Sadeq, A. H.,* Ultrasound-assisted desulfurization of crude oil using sodium hydroxide, J. Therm. Eng. **11** (2025) 1639. doi: https://doi.org/10.14744/thermal.0001030
19. *Volkova, G. I., Zubarev, D. A.,* Influence of processing conditions on the properties of high paraffin oil and sediment composition, Solid Fuel Chem. **58** (2024) 87. doi: https://doi.org/10.3103/S0361521924020149
20. *Ilyushin, Y. V.,* Development of a process control system for the production of high-paraffin oil, Energies **15** (2022) 6462. doi: https://doi.org/10.3390/en15176462
21. *Li, W., Huang, Q., Wang, W., Dong, X., Gao, X., Hou, L.,* Estimating the wax breaking force and wax removal efficiency of cup pig using orthogonal cutting and slip-line field theory, Fuel **236** (2019) 1529. doi: https://doi.org/10.1016/j.fuel.2018.09.132

22. *Wei, B.,* Recent advances on mitigating wax problem using polymeric wax crystal modifier, J. Pet. Explor. Prod. Technol. **5** (2015) 391.
doi: https://doi.org/10.1007/s13202-014-0146-6
23. *Lyu, R., Xia, T., Liang, C., Zhang, C., Li, Z., Wang, L., Wang, Y., Wu, M., Luo, X., Ma, J., Wang, C., Xu, C.,* MPEG grafted alkylated carboxymethyl chitosan as a high-efficiency demulsifier for O/W crude oil emulsions, Carbohydr. Polym. **241** (2020) 116309.
doi: https://doi.org/10.1016/j.carbpol.2020.116309
24. *Tinsley, J. F., Jahnke, J. P., Adamson, D. H., Guo, X., Amin, D., Kriegel, R., Saini, R., Dettman, H. D., Prud'home, R. K.,* Waxy gels with asphaltenes: Part 2 – Use of wax control polymers, Energy Fuels **23** (2009) 2065.
doi: https://doi.org/10.1021/ef800651d
25. *Ramirez-Corredores, M. M.,* Asphaltenes, 2017, pp. 41–222.
doi: https://doi.org/10.1016/B978-0-12-801225-3.00002-4
26. *Stratiev, D., Nikolova, R., Veli, A., Shishkova, I., Toteva, V., Georgiev, G.,* Mitigation of asphaltene deposit formation via chemical additives: A review, Processes **13** (2025) 141.
doi: https://doi.org/10.3390/pr13010141
27. *Vieira, L. C., Buchuid, M. B., Lucas, E. F.,* Effect of pressure on the performance of poly(ethylene–vinyl acetate) as wax deposition inhibitors by calorimetric method, J. Appl. Polym. Sci. **126** (2012) 143.
doi: https://doi.org/10.1002/app.35050
28. *Kumar, R., Voolapalli, R. K., Upadhyayula, S.,* Prediction of crude oil blends compatibility and blend optimization for increasing heavy oil processing, Fuel Process. Technol. **177** (2018) 309.
doi: https://doi.org/10.1016/j.fuproc.2018.05.008
29. *Abdullah, M. M. S., Al-Lohedan, H. A., Atta, A. M.,* Synthesis and application of amphiphilic ionic liquid based on acrylate copolymers as demulsifier and oil spill dispersant, J. Mol. Liq. **219** (2016) 54.
doi: https://doi.org/10.1016/j.molliq.2016.03.011
30. *Cendejas, G., Arreguín, F., Castro, L. V., Flores, E. A., Vazquez, F.,* Demulsifying super-heavy crude oil with bifunctionalized block copolymers, Fuel **103** (2013) 356.
doi: https://doi.org/10.1016/j.fuel.2012.08.029
31. *Liang, C., Liu, Q., Xu, Z.,* Dewatering bitumen emulsions using interfacially active organic composite absorbent particles, Energy Fuels **30** (2016) 5253.
doi: https://doi.org/10.1021/acs.energyfuels.6b00228
32. GOST 11858-66, Petroleum and petroleum products – Method for determination of asphalt–resin substances (asphaltenes and resins), Moscow, 1966.
33. GOST 11851-85, Oil—Method for determination of paraffin (wax), Moscow, 1985.
34. GOST 33-2016, Petroleum and petroleum products—Determination of kinematic and dynamic viscosity, Moscow, 2016.
35. ISO 3104, Petroleum products—Determination of kinematic viscosity and calculation of dynamic viscosity, Geneva, Switzerland, 2020.
36. GOST 1929-87, Petroleum products—Methods for determination of dynamic viscosity by rotational viscometer, Moscow, 1987.
37. ISO 3219-1, Rheology—Vocabulary and symbols for rotational and oscillatory rheometry, Geneva, Switzerland, 2021.
38. ISO 3219-2, Rheology—General principles of rotational and oscillatory rheometry, Geneva, Switzerland, 2021.
39. RD-1982. Petroleum products — Method for determination of pour point (harmonized with GOST 20287-91), Moscow.
40. GOST 20287-2023, Petroleum products — Methods for determination of yield and solidification temperatures, Moscow, 2023
41. *Martirosyan, A., Ilyushin, Y., Afanaseva, O., Kukharova, T., Asadulagi, M., Khloponina, V.,* Development of an oil field's conceptual model, Int. J. Eng. **38** (2025) 381.
doi: https://doi.org/10.5829/ije.2025.38.02b.12